NMR Spectroscopy

DOI: 10.1002/ange.201305475

Study of Intermolecular Interactions in the Corrole Matrix by Solid-State NMR under 100 kHz MAS and Theoretical Calculations**

Takeshi Kobayashi, Kanmi Mao, Piotr Paluch, Agnieszka Nowak-Król, Justyna Sniechowska, Yusuke Nishiyama, Daniel T. Gryko, Marek J. Potrzebowski, and Marek Pruski**

Recent progress in solid-state (SS)NMR spectroscopic methods based on fast magic angle spinning (MAS)[1] has enabled new opportunities for the structural study of small quantities (< 5 mg) of natural abundance samples. Utilizing through-space and through-bond polarization transfer, indirect detection of low-γ nuclei, and suitable homo- and heteronuclear decoupling, one- and two-dimensional (1D and 2D) spectra of such samples can be measured with excellent sensitivity and resolution.[2] However, determination of the short-range intermolecular order often remains elusive. Such analyses can be well-served by studying heteronuclear correlations that take advantage of the large chemical shift range of most low-γ nuclei (for example, ^{13}C or ^{15}N). Indeed, heteronuclear correlation (HETCOR) NMR spectroscopy and measurements of internuclear distances, often in concert with theoretical calculations, have provided structural details of complex hydrogen-bonded systems in chemistry and biology, blended materials, and host–guest pairs.[3] Still, intermolecular polarization transfers to low-γ nuclei are often hampered by low sensitivity. A promising solution to this challenge is offered by homonuclear ^1H–^1H 2D correlation methods, such as double-quantum (DQ)MAS[4] or spin-diffusion (NOESY-like) experiments,[5] provided that sufficient resolution is achieved in both dimensions. One of the possible approaches is the use of ^1H CRAMPS decoupling in concert with fast MAS to boost resolution in these experiments.[6] The recent development of ultrafast MAS (at 100 kHz and more[7]) provides access to appropriate ^1H resolution without RF decoupling.

Herein, we report the first application of ^1H 2D SSNMR measurements under MAS at 100 kHz, which are used in combination with indirectly detected $^1H\{^{13}C\}$ and $^1H\{^{15}N\}$ HETCOR experiments and theoretical calculations to scrutinize the interactions within a host–guest (HG) system consisting of 5,10,15-tris(pentafluorophenyl)corrole **1**, and toluene (Scheme 1).

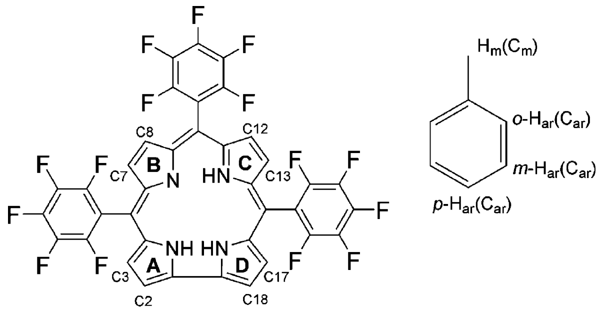

Scheme 1. Structures of 5,10,15-tris(pentafluorophenyl)corrole and toluene, with some of the notations used for peak assignments.

Corroles are aromatic macrocycles composed of four pyrrolic rings connected by three meso carbons and bearing one direct pyrrole–pyrrole link. The first synthesis of these materials was a multi-step process with low overall yield.[8] As synthetic methods have improved, there has been increased interest in potential applications of corroles in catalysis, sensors, imaging, and medicinal chemistry.[9] The coordination chemistry of corroles has attracted particular attention, and new metal–corrole systems possessing intriguing properties are being continuously reported.[10] Studies of solid-state structures of corroles and their interactions with other aromatic compounds pose challenges for diffraction and spectroscopic methods. Owing to the difficulties involved in growing X-ray quality crystals of the corroles, which tend to form disordered host(corrole)–guest(solvent) systems, only a few X-ray structures of unsubstituted metal-free corrole have been published to date, including that of corrole **1**.[11]

Herein, we present the results of $^1H\{^{13}C\}$ and $^1H\{^{15}N\}$ HETCOR experiments, the full interpretation of which could

[*] Dr. T. Kobayashi, Dr. K. Mao, Prof. M. Pruski
U.S. DOE Ames Laboratory, and
Department of Chemistry, Iowa State University
Ames IA, 50011 (USA)
E-mail: mpruski@iastate.edu

Dr. A. Nowak-Król, Prof. D. T. Gryko
Institute of Organic Chemistry, Polish Academy of Science
Kasprzaka 44/52, 01-224 Warsaw (Poland)

Dr. Y. Nishiyama
JEOL Resonance Inc.
3-1-2 Musashino, Akishima, Tokyo 196-8558 (Japan)

P. Paluch, J. Sniechowska, Prof. M. J. Potrzebowski
Centre of Molecular and Macromolecular Studies
Polish Academy of Science
Sienkiewicza 112, 90-363 Lodz (Poland)
E-mail: marekpot@cbm.lodz.pl

[**] This work was supported at Ames Laboratory by the U.S. Department of Energy, Office of Basic Energy Sciences under Contract No. DE-AC02-07CH11358, Grant of Polish National Center for Science, Contract No UMO-2011/03/N/ST4/01721 and The Foundation for Polish Science (A.N.-K. Ventures Program). We gratefully thank Dr. H.-H. Limbach, Dr. J. P. Yesinowski, and Dr. M. W. Schmidt for helpful discussions, and S. M. Althaus for assistance with solid-state NMR experiments.

Supporting information for this article, including sample preparation, solid-state NMR measurements, and theoretical calculations, is available on the WWW under http://dx.doi.org/10.1002/anie.201305475.

be made only with the help of theoretical calculations. The resulting ^{1}H chemical shift information is then used to analyze the highly resolved ^{1}H–^{1}H correlations, which provide the ultimate validation of the corrole–toluene HG structure.

We introduce the following notations (Scheme 1): nitrogen atoms in A–D rings are labeled as N_{A-D}; protons bonded to nitrogen atoms in A, C, and D rings are referred to as H_{NA}, H_{NC}, and H_{ND}; protonated carbons in **1** are denoted as C2, C3, and so on; methyl protons (carbons) in toluene are denoted as H_m (C_m); and aromatic protons (carbons) in positions *para-*, *meta-*, and *ortho-* are denoted as p-H_{ar} (p-C_{ar}), o-H_{ar} (o-C_{ar}), and m-H_{ar} (m-C_{ar}), respectively.

The static ^{1}H NMR spectrum (not shown) demonstrated that our HG system (including the toluene molecule) is rigid on the NMR timescale at about 300 K. The indirectly detected through-bond ^{1}H{^{13}C} HETCOR spectrum with polarization transfer via refocused INEPT (INEPTR-HETCOR)[2e] of the natural abundance HG system is shown in Figure 1 A. The dominant cross-peak at $\delta_H \approx -3.2$ ppm and $\delta_C \approx 14$ ppm is ascribed to correlation between H_m and C_m, [H_m, C_m]. Owing to host–guest interactions, both chemical shift values correspond to an increased shielding effect with respect to the solution NMR spectrum, where they would be present at around 2.2 ppm and 24 ppm, respectively (details are discussed later). A similar effect is observed in the aromatic ring of toluene. Because three H_{ar} resonances at $\delta_H \approx 1.4$, 0.8, and 0.1 ppm were easily resolved in 2D spectra taken at $\nu_R = 100$ kHz (Figure 2), we were able to assign the H_{ar}–C_{ar} correlations in Figure 1 A based on the build-up curves of the H_m–H_{ar} correlation signal (Supporting Information, Figure S2), to *para-*, *meta-*, and *ortho*-C–H pairs. The remaining cross-peaks are assigned to H–C correlations in **1** based on the computed ^{13}C chemical shifts as follows: **a**: H7–C7, H8–C8, **b**: H3–C3, H12–C12, H13–C13, and **c**: H2–C2, H17–C17, and H18–C18 (Supporting Information, Table S1). The ^{1}H{^{13}C} spectrum based on cross-polarization (CP-HETCOR) was consistent with these assignments (not shown).

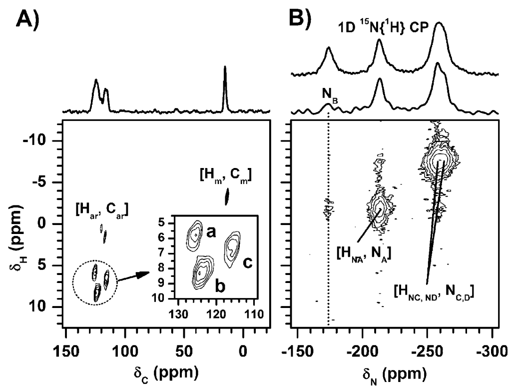

Figure 1. 2D indirectly detected ^{1}H{^{13}C} through-bond (A) and ^{1}H{^{15}N} through-space (B) HETCOR spectra of corrole **1** with toluene obtained at 14.1 T. A) $\nu_R = 40$ kHz, $\nu_{RF}(^{1}H) = 110$ kHz during short pulses, $\nu_{RF}(^{1}H) = 60$ kHz during tangent ramp CP, $\nu_{RF}(^{1}H) = 150$ kHz during homonuclear decoupling,[2e] $\nu_{RF}(^{1}H) = 20$ kHz during τ_{RR}, $\nu_{RF}(^{13}C) = 100$ kHz during short pulses and CP, $\nu_{RF}(^{13}C) = 10$ kHz during SPINAL-64 decoupling, $\tau_1 = 1.2$ ms, $\tau_2 = 1.3$ ms, $\tau_{CP} = 1$ ms, $\tau_{RR} = 40$ ms, 256 rows, 64 scans/row, $\Delta t_1 = 25$ μs, $\tau_{RD} = 1.5$ s, AT = 14.4 h. B) $\nu_R = 60$ kHz, $\nu_{RF}(^{1}H) = 100$ kHz during short pulses, $\nu_{RF}(^{1}H) = 54$ kHz during ramp CP, $\nu_{RF}(^{1}H) = 30$ kHz during τ_{RR}, $\nu_{RF}(^{15}N) = 114$ kHz during short pulses and CP, $\nu_{RF}(^{15}N) = 10$ kHz during SWFTPPM decoupling, $\tau_{CP} = 3$ ms, $\tau_{RR} = 80$ ms, 256 rows, 16 scans/row, $\Delta t_1 = 66.68$ μs, $\tau_{RD} = 3$ s, AT = 3.5 h. The symbols and further experimental details are explained in Supporting Information.

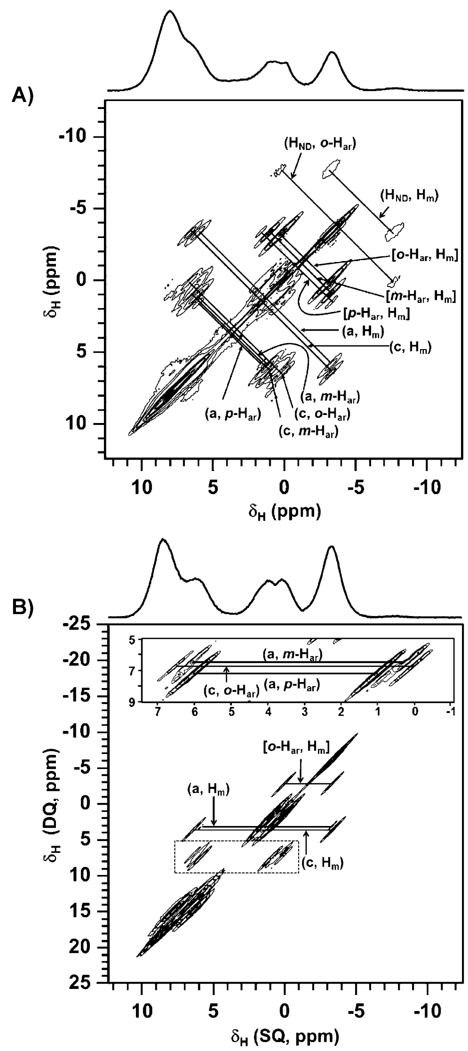

Figure 2. A), B) ^{1}H–^{1}H spin-diffusion and DQMAS spectra of corrole **1** with toluene, obtained at 14.1 T with $\nu_R = 100$ kHz, $\nu_{RF}(^{1}H) = 403$ kHz, $\tau_{RD} = 1.6$ s. Other experimental parameters: A) mixing time = 200 ms, 512 rows, 8 scans/row, $\Delta t_1 = 10$ μs, AT = 3.6 h; B) excitation and reconversion times = 0.1 ms, 512 rows, 32 scans/row, $\Delta t_1 = 10$ μs, AT = 14.5 h.

The indirectly detected ^{1}H{^{15}N} CP-HETCOR spectrum of ^{15}N-enriched **1** is shown in Figure 1 B, with the assignments based on the theoretically predicted ^{15}N chemical shifts (−233, −147, −264, and −259 ppm for N_A, N_B, N_C, and N_D, respectively, see Scheme 1 and Supporting Information for details). The well resolved ^{1}H–^{15}N cross-peaks demonstrate that no exchange among H_N protons (tautomerization) occurs in this system, at least at rates exceeding 1 kHz. The peak positions are similar to those observed in the close-to-freezing

(195 K) solution state (toluene) by Gross et al.,[11b] although our assignments for N_A and N_C are different. In the same study, the preferred tautomer was no longer observed at room temperature. In the HG system studied herein, the asymmetrically oriented pentafluorophenyl rings[11c] were immobilized on the NMR timescale (see the ^{19}F–^{19}F DQMAS spectrum in Supporting Information), which restricted tautomerization. The presence of guest molecules may have further inhibited the proton exchange.

Although the HETCOR experiments did not identify the HG intermolecular interactions directly, the obtained ^1H chemical shift information proved essential for the interpretation of the 2D ^1H–^1H spin-diffusion and DQMAS spectra acquired at $\nu_R = 100$ kHz without RF homonuclear decoupling (Figure 2). The spin-diffusion experiment yields diagonal peaks dominated by the non-exchanged magnetization and off-diagonal peaks associated with diffusive magnetization transfer within dipolar coupled networks of ^1H spins.[5] The ^1H–^1H DQMAS experiments reintroduce the MAS-averaged dipolar interactions. Signals representing pairs of coupled nuclei appear at the sum of their resonance frequencies in the indirect dimension, whereas autocorrelations from the non-coupled nuclei are removed by the DQ filter.[4]

The resolution in 2D spectra measured at $\nu_R = 100$ kHz is remarkable and proved essential in solving the structure of our HG system. In particular, the resonances ascribed to *p*-, *m*-, and *o*-H_{ar} were unresolved at $\nu_R = 40$ kHz (Figure 3 A,B). We also acquired a spectrum at $\nu_R = 40$ kHz using PMLG decoupling in both dimensions with windowed acquisition during t_2, yet both the resolution and the sensitivity proved inferior to 100 kHz MAS. A detailed account of this effort is given in Supporting Information. Note that the projections of 2D spectra in Figure 2 are broad in both dimensions with resolution similar to that observed in 1D MAS spectra taken at 40 kHz (Figure 3 C), showing that the line broadening is mainly inhomogeneous. The fact that the cross-peaks formed narrow ridges (especially in the DQMAS spectrum of Figure 2 B, which yields only short-range correlations) implies that the distributions of chemical shifts of interacting sites are correlated within crystallites with short-range order. The cross-peaks are extended along the diagonal (SQ-SQ in spin-diffusion or SQ-DQ in DQMAS), owing to constant chemical shift difference within each interacting pair, which suggests that the distributions may result from local anisotropic magnetic susceptibilities (not averaged by MAS[12]) rather than structural disorder or π–π stacking. In the latter scenarios, changes in local environments would be less dependent of each other, leading to round or "bent" correlation peaks, as observed in disordered organic solids.[12a,13] It is known that homogeneous ^1H–^1H dipolar broadening scales down linearly with increasing ν_R. The cross-sections in Figure 3 C (slices I–III) show that MAS at 100 kHz reduced it to less than 0.2 ppm (see also insets in Figure 2 B; note that the exact measure of homogeneous broadening is given by the line width along the antidiagonal). The increased width of cross-peaks in Figure 3 A is due to ^1H spin diffusion, which transports magnetization between crystallites with different local fields.

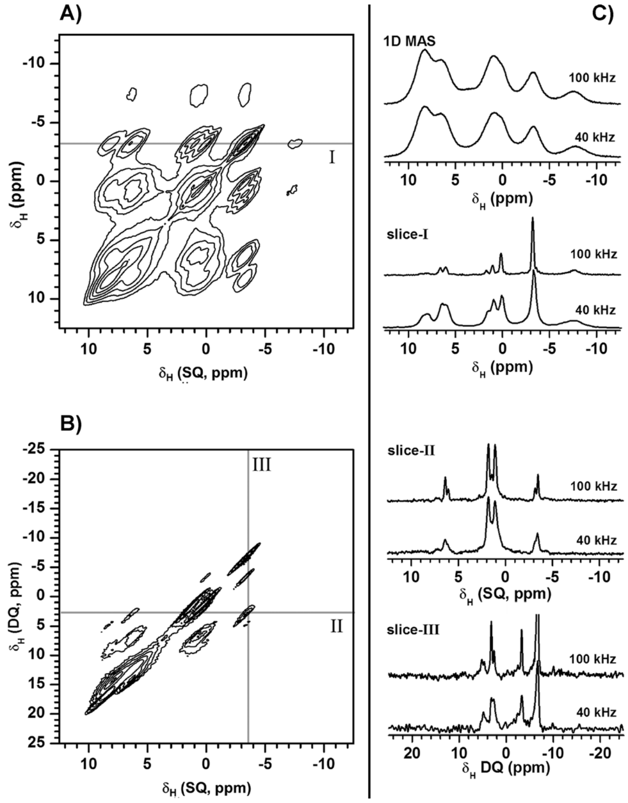

Figure 3. A), B) ^1H–^1H spin-diffusion and DQMAS spectra of corrole **1** with toluene, obtained at 14.1 T with $\nu_R = 40$ kHz, $\nu_{RF}(^1H) = 125$ kHz and $\tau_{RD} = 1.6$ s. Other experimental parameters: A) mixing time = 100 ms, 128 rows, 8 scans/row, $\Delta t_1 = 50$ μs, AT = 0.9 h; B) excitation and reconversion times = 0.1 ms, 128 rows, 16 scans/row, $\Delta t_1 = 25$ μs, AT = 1.8 h. C) 1D ^1H MAS spectra at $\nu_R = 40$ kHz (bottom) versus 100 kHz (top), and slices of spin-diffusion and DQMAS spectra from Figure 2 taken at the positions indicated by gray lines.

The spectra of Figure 2 show numerous intra- and intermolecular correlations. The intramolecular assignments are not marked, except for those associated with H_m, which are shown using square brackets ([,]) to illustrate the outstanding resolution achieved under MAS at 100 kHz. The remaining cross-peaks denote correlations between ^1H nuclei previously assigned to the host (**a**, **b**, **c**, and H_{ND}) and the guest (H_m, *o*-H_{ar}, *m*-H_{ar}, and *p*-H_{ar}). In the spin-diffusion spectrum, the strongest HG correlations include (**a**, H_m), (**a**, *m*-H_{ar}), (**a**, *p*-H_{ar}), (**c**, H_m), (**c**, *o*-H_{ar}), (**c**, *m*-H_{ar}), (H_{ND}, *o*-H_{ar}), and (H_{ND}, H_m). The DQMAS spectrum in Figure 2 B features a subset of these cross-peaks corresponding to short-range dipolar coupled pairs: (**a**, H_m), (**a**, *m*-H_{ar}), (**a**, *p*-H_{ar}), (**c**, H_m), and (**c**, *o*-H_{ar}). Only faint cross-peaks between **b** and protons of toluene were observed in the two spectra.

Based on the observed intensities of NMR cross-peaks, an HG structure emerges whereby toluene is intercalated between the corroles such that the methyl group points toward the D ring, while the *p*-H_{ar} is close to the B ring. This result is in agreement with the structure of the HG complex optimized by DFT calculations, in which the aromatic ring of toluene is sandwiched between two tetrapyrrolic rings in almost parallel fashion with about 3.5 Å of separation (see

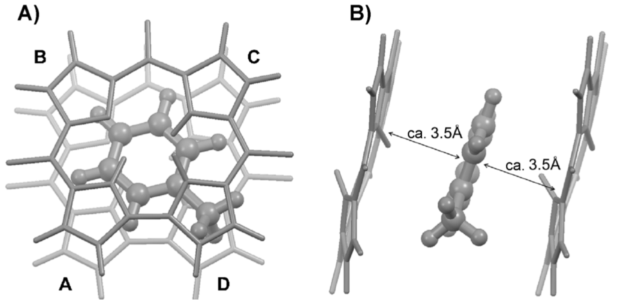

Figure 4. The computed position of toluene in the corrole–toluene system. Pentafluorophenyl rings are omitted for clarity.

Figure 4 and Supporting Information). Most likely, the toluene molecule is encapsulated through π–π interactions in the host matrix[14] and the large upfield shifts result from a strong ring current effect that is due to the delocalized π-electrons on the corrole macrocycle. A similar HG system has been previously observed in a bis(porphyrin)–pyrene system,[15] in which the pyrene was sandwiched between porphyrin rings through π–π interactions and the pyrene protons were shifted to the upfield region by the ring current effect. Other corroles containing more electron-rich substituents may form similar aggregates, possibly with larger aromatic guests.

In summary, MAS at 100 kHz and theoretical calculations provided decisive information about the host–guest interactions between electron-deficient corrole and toluene, including the specific molecular orientation. This kind of approach adds another method for studying intermolecular interactions in increasingly complex structures ("NMR crystallography"), especially in cases where diffraction methods are impeded by the lack of long-range order or difficulty in obtaining crystals of sufficient quality. In a more general sense, MAS at 100 kHz and more will provide new opportunities to increase resolution in 2D homo- and heteronuclear spectra of a variety of systems in biology,[7b] chemistry, and materials science.

Received: June 26, 2013
Revised: October 4, 2013
Published online: November 13, 2013

Keywords: corroles · host–guest interactions · solid-state NMR spectroscopy · theoretical calculations · ultrafast MAS

[1] A. Samoson, T. Tuherm, J. Past, A. Reinhold, T. Anupold, I. Heinmaa in *New Techniques in Solid-State Nmr*, *Vol. 246* (Ed.: J. Klinowski), Springer-Verlag, Berlin–Heidelberg, **2004**, pp. 15–31.

[2] a) Y. Ishii, R. Tycko, *J. Magn. Reson.* **2000**, *142*, 199–204; b) J. W. Wiench, C. E. Bronnimann, V. S. Y. Lin, M. Pruski, *J. Am. Chem. Soc.* **2007**, *129*, 12076–12077; c) E. Vinogradov, P. K. Madhu, S. Vega, *Chem. Phys. Lett.* **1999**, *314*, 443–450; d) B. Elena, A. Lesage, S. Steuernagel, A. Bockmann, L. Emsley, *J. Am. Chem. Soc.* **2005**, *127*, 17296–17302; e) K. Mao, M. Pruski, *J. Magn. Reson.* **2009**, *201*, 165–174.

[3] a) M. Schulz-Dobrick, T. Metzroth, H. W. Spiess, J. Gauss, I. Schnell, *ChemPhysChem* **2005**, *6*, 315–327; b) J. R. Yates, T. N. Pham, C. J. Pickard, F. Mauri, A. M. Amado, A. M. Gil, S. P. Brown, *J. Am. Chem. Soc.* **2005**, *127*, 10216–10220; c) G. Zucchi, P. Viville, B. Donnio, A. Vlad, S. Melinte, M. Mondeshki, R. Graf, H. W. Spiess, Y. H. Geerts, R. Lazzaroni, *J. Phys. Chem. B* **2009**, *113*, 5448–5457.

[4] a) M. Feike, D. E. Demco, R. Graf, J. Gottwald, S. Hafner, H. W. Spiess, *J. Magn. Reson. Ser. A* **1996**, *122*, 214–221; b) S. P. Brown, *Macromol. Rapid Commun.* **2009**, *30*, 688–716.

[5] S. P. Brown, *Prog. Nucl. Magn. Reson. Spectrosc.* **2007**, *50*, 199–251.

[6] a) P. K. Madhu, E. Vinogradov, S. Vega, *Chem. Phys. Lett.* **2004**, *394*, 423–428; b) S. P. Brown, A. Lesage, B. Elena, L. Emsley, *J. Am. Chem. Soc.* **2004**, *126*, 13230–13231.

[7] a) Y. Nishiyama, Y. Endo, T. Nemoto in *53rd ENC*, Miami, FL, USA, **2012**; b) B. H. Meier, A. Samoson, A. Bockmann, M. Ernst, V. Agarval, M. Huber, F. Ravotti, J. Gath in *54th ENC*, Pacific Grove, California, USA, **2013**.

[8] A. W. Johnson, I. T. Kay, *Proc. Chem. Soc. London* **1964**, 89–90.

[9] a) I. Aviv, Z. Gross, *Chem. Commun.* **2007**, 1987–1999; b) D. T. Gryko, *J. Porphyrins Phthalocyanines* **2008**, *12*, 906–917; c) R. Paolesse, *Synlett* **2008**, 2215–2230; d) I. Aviv-Harel, Z. Gross, *Chem. Eur. J.* **2009**, *15*, 8382–8394; e) A. B. Alemayehu, E. Gonzalez, L. K. Hansen, A. Ghosh, *Inorg. Chem.* **2009**, *48*, 7794–7799.

[10] a) A. M. Albrett, J. Conradie, P. D. W. Boyd, G. R. Clark, A. Ghosh, P. J. Brothers, *J. Am. Chem. Soc.* **2008**, *130*, 2888–2889; b) J. H. Palmer, A. C. Durrell, Z. Gross, J. R. Winkler, H. B. Gray, *J. Am. Chem. Soc.* **2010**, *132*, 9230–9231; c) A. B. Alemayehu, A. Ghosh, *J. Porphyrins Phthalocyanines* **2011**, *15*, 106–110; d) L. M. Reith, M. Himmelsbach, W. Schoefberger, G. Knoer, *J. Porphyrins Phthalocyanines* **2011**, *15*, 247–253; e) H. L. Buckley, M. R. Anstey, D. T. Gryko, J. Arnold, *Chem. Commun.* **2013**, *49*, 3104–3106.

[11] a) Z. Gross, N. Galili, I. Saltsman, *Angew. Chem.* **1999**, *111*, 1530–1533; *Angew. Chem. Int. Ed.* **1999**, *38*, 1427–1429; b) Y. S. Balazs, I. Saltsman, A. Mahammed, E. Tkachenko, G. Golubkov, J. Levine, Z. Gross, *Magn. Reson. Chem.* **2004**, *42*, 624–635; c) T. Ding, J. D. Harvey, C. J. Ziegler, *J. Porphyrins Phthalocyanines* **2005**, *9*, 22–27.

[12] a) D. L. Vanderhart, W. L. Earl, A. N. Garroway, *J. Magn. Reson.* **1981**, *44*, 361–401; b) U. Schwerk, D. Michel, M. Pruski, *J. Magn. Reson. Ser. A* **1996**, *119*, 157–164.

[13] D. Sakellariou, S. P. Brown, A. Lesage, S. Hediger, M. Bardet, C. A. Meriles, A. Pines, L. Emsley, *J. Am. Chem. Soc.* **2003**, *125*, 4376–4380.

[14] C. A. Hunter, J. K. M. Sanders, *J. Am. Chem. Soc.* **1990**, *112*, 5525–5534.

[15] A. Chaudhary, S. P. Rath, *Chem. Eur. J.* **2011**, *17*, 11478–11487.

